JOC The Journal of Organic Chemistry

Article

Kinetics of Electrophilic Alkylations of Barbiturate and Thiobarbiturate Anions

Alexander Schade, Ivan Tchernook, Mirko Bauer, Alexander Oehlke, Martin Breugst, Joachim Friedrich, and Stefan Spange

J. Org. Chem., **Just Accepted Manuscript** • DOI: 10.1021/acs.joc.7b01223 • Publication Date (Web): 17 Jul 2017

ACS Publications

The Journal of Organic Chemistry is published by the American Chemical Society. 1155 Sixteenth Street N.W., Washington, DC 20036

Kinetics of Electrophilic Alkylations of Barbiturate and Thiobarbiturate Anions

Alexander Schade[‡], Ivan Tchernook[†]*, Mirko Bauer[‡], Alexander Oehlke[‡], Martin Breugst[§], Joachim Friedrich[†] and Stefan Spange[‡]*

[‡]*Department of Polymer Chemistry, Technische Universität Chemnitz, Straße der Nationen 62, 09107 Chemnitz, Germany*, [†]*Department of Theoretical Chemistry, Technische Universität Chemnitz, Straße der Nationen 62, 09107 Chemnitz, Germany* and [§]*Department für Chemie, Universität zu Köln, 50939 Köln, Germany.*

stefan.spange@chemie.tu-chemnitz.de

RECEIVED DATE (will be automatically inserted after manuscript is accepted).

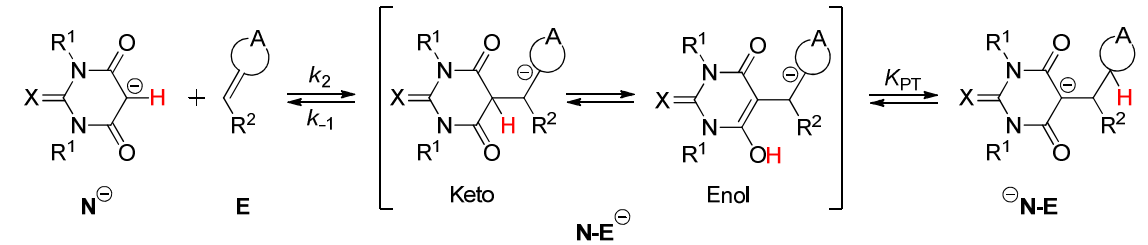

B: R^1 = H; X = O
SB: R^1 = H; X = S
MB: R^1 = Me; X = O
ESB: R^1 = Et; X = S

R^2 = Donor Substituent
A = Acceptor Group

K_{PT} = Equilibrium of the Proton-Transfer-Reaction

Abstract: Second-order rate constants (k_2) of the reactions of various barbiturate anions such as the parent barbiturate, 1,3-dimethylbarbiturate, 2-thiobarbiturate, and 1,3-diethyl-2-thiobarbiturate with diarylcarbenium ions and Michael acceptors have been determined in dimethylsulfoxide solution at 20 °C. The reactivity parameters N and s_N of the barbiturate anions were derived from the linear plots of log k_2 versus the electrophilicity parameters E of these reference electrophiles, according to the linear-free-energy relationship log k_2 (20 °C) = s_N (E+N). Several reactions of these nucleophiles with benzylidenemalononitriles and quinone methides proceeded with reversible formation of the new C–C-bond followed by rate-determining proton shift. No evidence for initial attack of the electrophiles at the enolate oxygens of these nucleophiles was found by the kinetic measurements, in line with quantum chemical DFT calculations, which showed that in all cases C-attack is kinetically and

thermodynamically preferred over O-attack. The nucleophilic reactivities of barbiturate anions were compared with those of structurally related carbanions, e.g., Meldrum's acid and dimedone anions.

Introduction

Barbituric acid (BA) derivatives are important for medical applications due to their anxiolytic and hypnotic properties.[1] Furthermore, certain barbiturate derivatives such as murexide[2] are analytically relevant complex ligands or suitable as NLO (non-linear optics) chromophores and solvatochromic dyes.[3-5]

The parent BA is a CH-acidic compound which belongs to the class of malonic acid derivatives.[6] Accordingly, 5-unsubstituted BA derivatives undergo Knoevenagel condensation reactions,[7-10] which give benzylidene derivatives with benzaldehydes.[11] Structurally related *push-pull* dyes, with the BA moiety as electron acceptor substituent, are available by reactions of BA anions with benzhydrylium cations followed by an oxidation reaction [Scheme 1 (a)].[9]

Another type of barbituric acid dyes is available by nucleophilic aromatic substitution of EWG (electron withdrawing group) *para*-substituted aromatic fluoro compounds with barbiturate anions [Scheme 1 (b)].[12] Such barbiturate dyes can switch between the keto- and enol-form depending on the environment.[12,13] The enol formation is associated with a color development because a *push-pull* dye is generated with the barbiturate substituent as electron donating group (EDG).[12,13] Accordingly, the BA moiety can serve either as EWG (a) or EDG (b) as illustrated in Scheme 1.

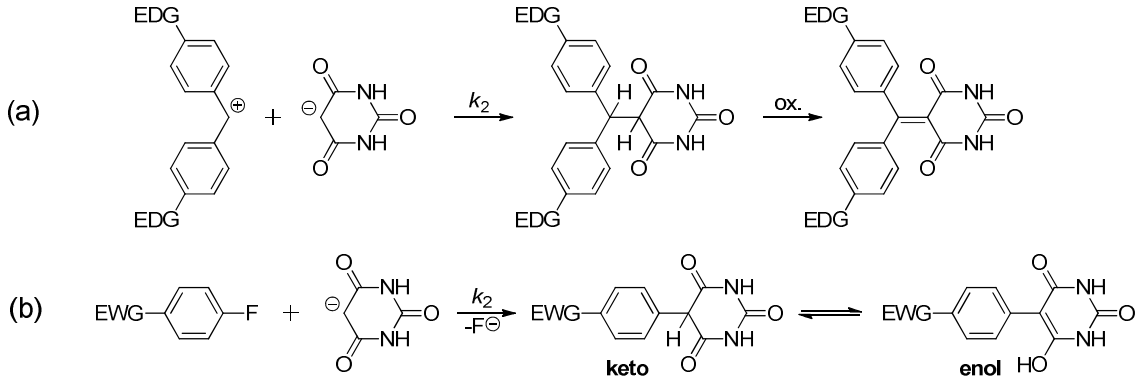

Scheme 1. Two examples of reactions of barbiturate anions with organic electrophiles to produce solvatochromic dyes. EDG = electron donating group; EWG = electron withdrawing group.

Therefore, barbiturate dyes are useful as switchable chromophores with fluctuating hydrogen bonding pattern [Scheme 1 (b)].[12,13] This feature provides the BA moiety as

valuable substituent for manifold applications in molecular recognition of nucleic bases and related compounds.[9,12,13] Usually, the BA moiety is introduced by the synthetic procedures illustrated in Scheme 1, where the barbiturate anion undergoes a nucleophilic attack on the electrophilic carbon atom of the substrate. A successful synthesis significantly depends on the nucleophilic reactivity of *C*-5 of the barbiturate anion in conjunction with an appropriate electrophilic reagent. However, competition between *C*-, *O*-, and *N*-alkylation has to be considered when BA anions undergo reactions with electrophiles (Scheme 2). For example, products arising from *C*-attack were obtained in reactions with carbonyl compounds.[14,15] Alkylations with dication ethers,[16,17] alkyl iodides,[18] dimethyl sulfate[19] or diazomethane[20] yield mixtures of *C*-, *O*-, and *N*-alkylated products of BA. *N*-alkylated products are solely formed by reactions of 5,5-dialkylsubstituted BA with triphenylmethylium ions.[21,22]

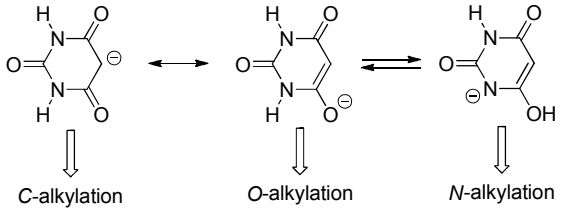

Scheme 2. Examples of resonance structures and tautomerism of barbituric acid anion which demonstrate the possible nucleophilic centers of those nucleophiles.

Whereas acid properties of BA derivatives were studied in water and DMSO,[23-25] quantitative data on nucleophilic reactivity of barbiturate anions are still not reported compared to well characterized malonic acid and meldrum's acid derivatives.[26,27]

As the pK_a-values of CH-acids correlate only poorly with the nucleophilicity of the corresponding carbanions,[28] reactivity parameters of barbiturates must be attained by studying their kinetics with reference electrophiles.

A methodology had been established to derive the nucleophilic reactivities of carbanions from the second-order rate constants of their reactions with reference electrophiles. It has been shown that the second-order rate constants (k_2) can be calculated from the nucleophilicity parameter N, the nucleophile-specific susceptibility parameter s_N, and the electrophilicity parameter E (eq. 1).[28-38]

$$\log k_2\ (20\ °C) = s_N\ (N + E) \qquad (1)$$

This study aims to investigate the kinetics of barbituric- and thiobarbituric acid salts as well as their 1,3-dialkylated derivatives (Scheme 3) with various electrophilic compounds in order to obtain quantitative information about their nucleophilicity (N) according to eq. 1.

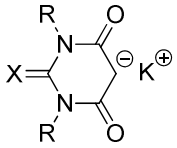

B: R = H; X = O
SB: R = H; X = S
MB: R = Me; X = O
ESB: R = Et; X = S

Scheme 3. Barbiturate anions used in this work.

Results

The nucleophilicities of barbiturate anions were determined by studying the kinetics of their reactions with benzhydrylium ions **1c–g** and Michael acceptors **2–6** (Table 1) as reference electrophiles, which differ highly in reactivity whereas the steric shielding of the reaction center is not varied significantly.[39]

Table 1. Electrophilicity parameters (E) and UV/vis absorption maxima of benzhydrylium ions **1a–g** and Michael acceptors **2–6** employed as reference electrophiles in this study.

cationic electrophiles				E[b]	λ_{max}[c] [nm]
	**1**	**a**:	R^1 = 	+3.63	469[a]
		b:	R^1 = 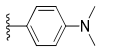	–7.02	613[a]
		c:	R^1 = 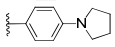	–7.69	620
		d:	R^1 = 	–8.22	618
		e:	R^1 = 	–8.76	627
		f:	R^1 = 	–9.45	635
		g:	R^1 = 	–10.04	630

neutral Michael acceptor electrophiles				E[b]	λ_{max}[c] [nm]
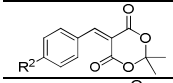	**2**	**a:**	R^2 = H	–9.15	325
		b:	R^2 = MeO	–10.28	366
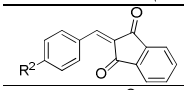	**3**	**a:**	R^2 = MeO	–11.32	388
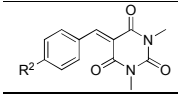	**4**	**a:**	R^2 = Me_2N	–12.76	480
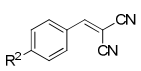	**5**	**a:**	R^2 = H	–9.42	311
		b:	R^2 = MeO	–10.80	354
		c:	R^2 = Me_2N	–13.30	441
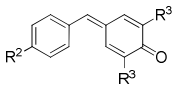	**6**	**a:**	R^2 = MeO; R^3 = Ph	–12.18	422
		b:	R^2 = Me_2N; R^3 = Ph	–13.39	533
		c:	R^2 = Me; R^3 = ^{t}Bu	–15.83	371

a) electrophiles used only for product studies
b) electrophilicity parameters were taken from refs [11,40-45]
c) λ_{max}-values were taken from refs [11,28,41,42,44]

The barbiturate salts shown in Scheme 3 were generated by treating the corresponding barbituric acids with aqueous solutions of stoichiometric amounts of K_2CO_3 or tetra-*n*-butylammonium hydroxide. The potassium salts **B** and **SB** (Scheme 3) precipitated, were separated by filtration, washed with cold water, and dried under reduced pressure. The potassium salts **MB** and **ESB** were isolated by evaporation of water and subsequent recrystallization of the crude products from ethanol. The tetra-*n*-butylammonium salt (**NBu_4MB**) was isolated by removing water and recrystallization of the crude product from diethyl ether.

NMR-product studies

One purpose of the various NMR-studies was to prove whether *O*-, *C*- or *N*-reactivity of the barbiturate anions with the different types of electrophiles was kinetically observed. Therefore, according to previous studies,[11,41,42,46] the reaction of at least one nucleophile with one example of each type of electrophiles, was directly monitored by NMR-experiments in d_6-DMSO. Selected representative products were isolated for full product characterization.

Benzhydrylium ion **1a** was chosen as electrophile for the product studies because a potentially kinetically preferred *O*-alkylation product would be expected due to the high electrophilicity of **1a** according to ref. [47].

However, only *C*-alkylation products were produced by reactions of both benzhydrylium cations (**1a** and **1b**) with **MB** (Scheme 4).[9] For details and spectroscopic data see Experimental Section or Supporting Information page S20 – S29.

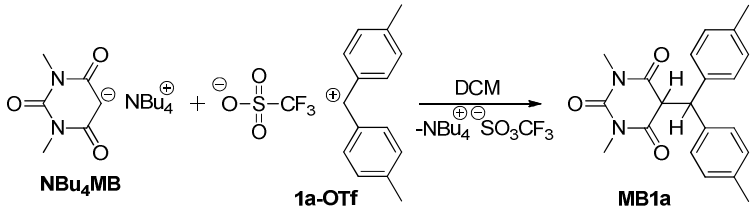

Scheme 4. Reaction of **NBu_4MB** with **1a-OTf**, directly monitored via ^{1}H NMR experiments.

The observed reaction cascade of **MB** with **2b**, which course is similar to that of **SB** with **4a**, is illustrated in Scheme 5. The initial C−C-bond formation is reversible for these nucleophile-electrophile combinations. Subsequently, the negatively charged intermediates can undergo an intramolecular proton transfer (Scheme 5) and two different species are in

equilibrium: an anion with the negative charge on the former electrophile part **N–E**$^{\ominus}$ and an anion with the negative charge on the former nucleophile part $^{\ominus}$**N–E** (Scheme 5). Together with the equilibrium between **N–E**$^{\ominus}$ and $^{\ominus}$**N–E** (Scheme 5), the formation of the anion of Meldrum's acid (**MA**) and 5-(4-methoxybenzylidene)-1,3-dimethylbarbiturate (**4b**) are possible by C−C-bond cleavage of the secondary product $^{\ominus}$**N–E**.

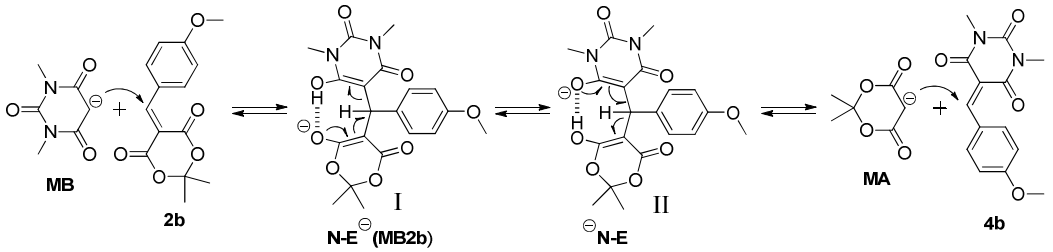

Scheme 5. Equilibria observed during reaction of **MB** and **2b** as directly monitored by ^{1}H NMR-experiment in DMSO.

Hence, not only the initially formed and assumed asymmetric adduct (**MB2b**) could be observed during the reaction. Two symmetric products were also found (Scheme 6) due to reactions of the additionally generated nucleophile (**MA**) and electrophile (**4b**). The products were identified NMR-spectroscopically by three singlet signals for **MB+2b** at 5.07 ppm, 5.61 ppm and 6.12 ppm and for **SB+4a** at 5.96 ppm, 6.08 ppm and 6.20 ppm with statistically determined integrals of 0.25 : 0.50 : 0.25. Complete ^{1}H NMR-spectroscopic data are given in the Experimental Part.

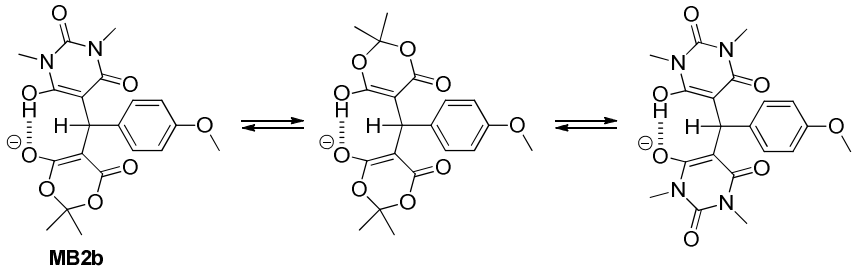

Scheme 6. Found product mixture in the ^{1}H-NMR-experiment of reaction of **MB** with **2b** in DMSO.

For the reaction of **3a** with **MB**, the back reaction is very slow, thereby the initially formed asymmetric product could be identified. The formation of the symmetric byproducts were detected in the ^{1}H-NMR spectra after >48 hours. **N–E**$^{\ominus}$ seems to be stabilized by tautomerization towards the enolic-form of the barbiturate moiety and formation of an intramolecular hydrogen bond as illustrated for **MB3a** in Scheme 7 (results from ^{1}H NMR spectroscopy are given in the Experimental Section). A singlet at 5.61 ppm is detected in the

^{1}H NMR-spectrum for the central CH-group which indicates the formation of **MB3a** (Scheme 7).

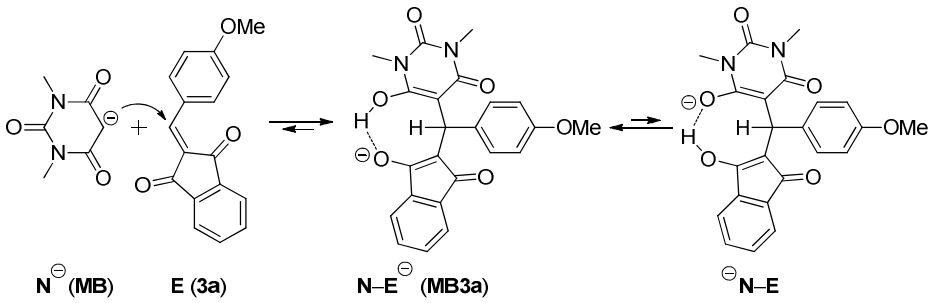

Scheme 7. Reaction of **MB** with **3a** as directly monitored by ^{1}H NMR-experiment in DMSO.

^{1}H NMR-studies of products formed from alkylidene malononitriles (**5**) with **MB** in DMSO show two doublets at 4.68 and 6.20 ppm for **MB5a** and at 4.57 and 6.10 ppm for **MB5c** (Scheme 8). This is an indication that these products do not form an intramolecular hydrogen bond (Scheme 8). The initially formed adducts **N–E**$^{\ominus}$ were transferred into the barbiturate anions $^{\ominus}$**N–E**, as shown in Scheme 8. In case of the reaction of **MB** with **5a**, the product **MB5aH** could be isolated after treating the mixture with trifluoroacetic acid. Analogous products have previously been observed for the reactions of benzylidenemalononitriles with carbanions of *β*-diketones[42] and of benzylidenebarbiturates with malononitrile anions.[11] However, the intermediate **MB5c** decomposes to portions of **5c** and 1,3-dimethylbarbituric acid if trifluoroacetic acid is added.

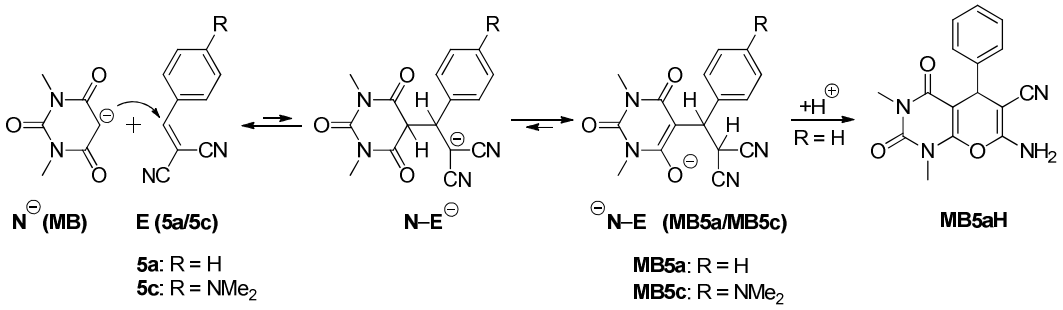

Scheme 8. Suggested reaction cascade of **MB** with **5a** and **5c** as directly monitored by ^{1}H NMR-experiment in DMSO. Product **MB5aH** could be isolated as solid in 76% yield (see experimental part).

The phenol intermediate (**MB6c**) was observed for the reaction of the quinonemethide **6c** with **MB**. The product formation is explainable by C-alkylation with a subsequent proton transfer reaction (Scheme 9). **MB6cH** could be isolated in 88 % yield after treating the mixture with trifluoroacetic acid.

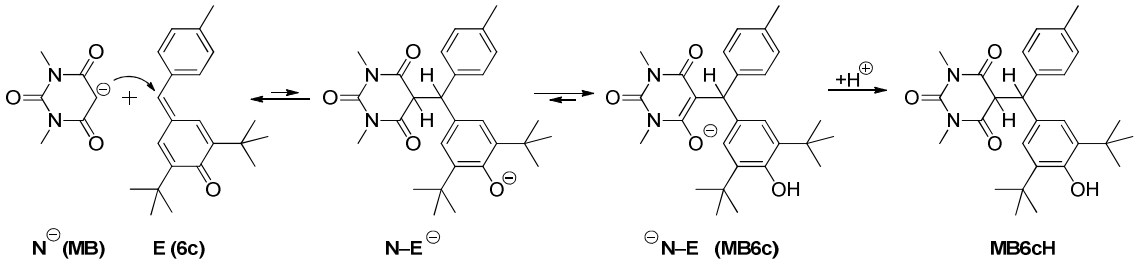

Scheme 9. Suggested reaction cascade of **MB** with **6c** as directly monitored by ^{1}H NMR-experiment in DMSO. Product **MB6aH** could be isolated in 88% yield (see experimental part).

Because of the better solubility, **MB** was chosen as nucleophile for most of the product characterizations. To study the influence of *N*-alkylation, an ^{1}H NMR experiment of **B** with **6c** in d_6-DMSO was performed. A singlet at 5.21 ppm was detected, which is characteristic for the central CH-group, occurring after C−C-bond formation (see Experimental Section). *N*-alkylation is therefore not observed for the unalkylated barbituric acid anions **B** and **SB**.

Altogether, only products resulting from *C*-alkylation were found for all nucleophile-electrophile combinations as proven by ^{1}H NMR spectroscopy. Spectroscopic data are given in the experimental part.

It could be concluded from the product studies that the initially formed intermediates **N–E**$^{\ominus}$ may undergo a proton shift to form $^{\ominus}$**N–E** (keto- or enol-structure) (Scheme 10). The relative concentrations of these types of adducts were controlled by the acid-base equilibrium constant K_{PT} (Scheme 10).[48]

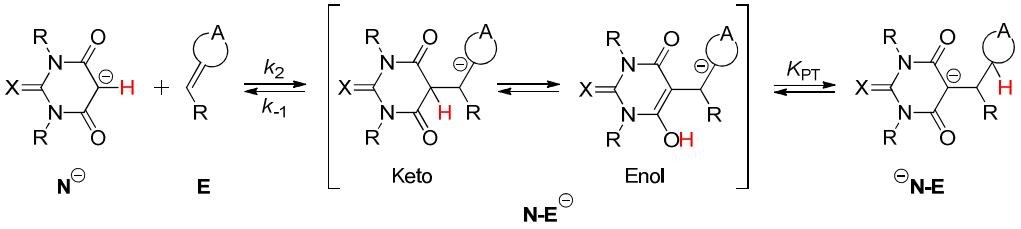

Scheme 10. Suggested scenario for the reactions of the barbiturate anion (**N**$^{\ominus}$) with neutral Michael acceptors (**E**).

Generally, the scenario suggested in Scheme 10 applies to all barbiturate anion/Michael acceptor combinations which have to be considered by interpreting the kinetic data.

Kinetic investigations

The kinetics of the reactions of barbiturate anions (Scheme 3) with reference electrophiles (Table 1) were studied in DMSO solution at 20 °C by monitoring the UV/vis

absorptions of the electrophiles by means of conventional or stopped-flow techniques. To simplify the evaluation of the kinetic experiments, the barbiturate anions were used in large excess (> 10 equiv.). Thus their concentrations remained almost constant throughout the reactions, and pseudo-first-order rate constants were obtained in all runs. The observed first-order-rate constants (k_{obs}) were derived by least squares fitting of the exponential function $A_t = A_0 \times \exp(- k_{obs} \times t) + C$ to the time dependent absorbances A_t of the electrophiles (Figure 1). Second-order-rate constants (k_2) were obtained as the slopes of linear correlations of k_{obs} with the concentrations of the nucleophiles (Figure 1) The axis interception is the sum of all side reactions, including the back reaction k_{-1} as shown in Figure 2. All data are listed in Table 2.

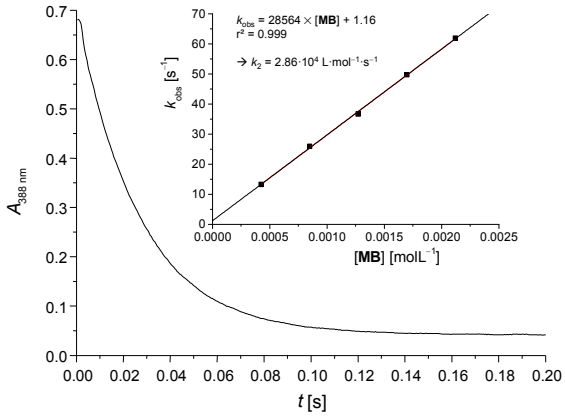

Figure 1. Plot of the UV/vis absorbance of **3a** ($c = 4.45 \times 10^{-5}$ molL^{-1}) versus time for its reaction with **MB** ($c = 1.27 \times 10$–3 molL–1) in DMSO at 20 °C; inset: correlation of the pseudo-first-order rate constants (k_{obs}) versus concentration of **MB**.

Figure 2 illustrates the incomplete reaction of the barbituric acid based Michael acceptor **4a** with **MB**. The obtained k_{obs} values increase linearly with the nucleophile concentration with a slope corresponding to the second-order rate constant of the forward reaction and an intercept, which indicates the incomplete conversion for combinations of **MB**+**3a**, **SB**+**3a**, **ESB**+**3a**, **B**+**4a**, **MB**+**4a**, **SB**+**4a** and **ESB**+**4a** (see SI page S9−S11).[49] Also negative intercepts were found, which could be related to a partial decomposition of the nucleophile during dissolution as suggested in the literature.[50] However, self-aggregation or strong solvation of the barbiturate anions by DMSO may also possible because of their high dipolarity. But, these negative intercepts are small and, because of the good correlation of log k_2 versus electrophilicity (E) of these data, they were further used for the determination of the nucleophilicity (N) of barbiturate anions.

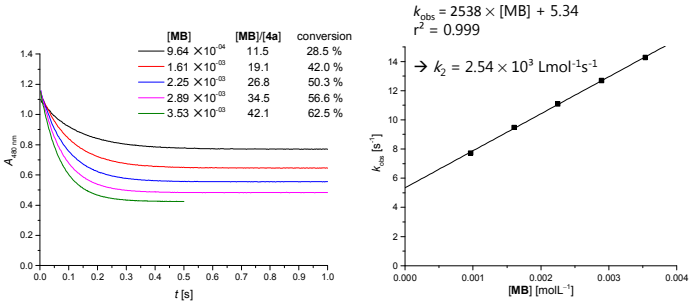

Figure 2. left: Plot of the UV/vis absorbances of **4a** versus time for five different concentrations of **MB** in DMSO at 20 °C; right: plot of the obtained pseudo-first-order rate constants (k_{obs}) versus the nucleophile concentration.

Altogether, reactions of barbiturate anions with electrophiles **3a** and **4a** show incomplete conversions. The degree of conversion increases in the order from oxo- to thiobarbiturates (**B** < **SB** and **MB** < **ESB**) and from alkylated to nonalkylated barbiturates (**MB** < **B** and **ESB** < **SB**) as measured by UV/vis spectroscopy (see SI page S9 – S11).

The equilibrium constants (K) are identified by titration experiments according to Figure 2 left, by measuring the incomplete conversions of the electrophile at the equilibrium state for reactions of **B**, **MB**, **SB** and **ESB** with the electrophiles **3a** and **4a** (see Table S1). Reaction rate constant of the back reaction (k_{-1}) from ordinary intercept are determined to check the magnitude of the K-value (Scheme 11). Data and discussion see supporting information page S1 – S2.

The interpretation of the observed second-order-rate constants ($k_{2,obs}$) is unambiguous in cases where the initial C–C-bond-forming step immediately yields the final product. The situation is more complex, when the observable product is formed through a proton transfer following the C–C-bond-forming step which may play a role according to the product studies observed for the electrophiles of the **5-** and **6**-type.

If the Bodenstein approximation (steady state of the initially formed adduct) can be applied for the reaction sequence in Scheme 11, the rate of disappearance of the electrophile is given by eq. 3.[51-53] For a detailed mathematic derivation of eq. 3 see Supporting Information page S16. Scheme 11 does not consider the additional keto-enol equilibria for simplification.

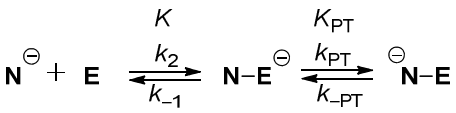

Scheme 11. General reaction scheme of an anionic nucleophile $\mathbf{N}^{\ominus}$ with a neutral electrophile **E**.

$$\frac{\mathrm{d[E]}}{\mathrm{d}t} = -k_2 \times [\mathrm{E}]\,[\mathrm{N}^-] \times \frac{k_{\mathrm{PT}}}{k_{\mathrm{PT}} + k_{-1}} \quad (3)$$

Let us now consider two extremes for the relative magnitudes of the reverse reaction (k_{-1}) and the proton transfer k_{PT} (eq. 4 and 5)

$$\text{for } k_{\mathrm{PT}} \gg k_{-1} \Rightarrow \frac{\mathrm{d[E]}}{\mathrm{d}t} = -k_2 \times [\mathrm{E}]\,[\mathrm{N}^-] \quad \text{(fast proton transfer)} \quad (4)$$

$$\text{for } k_{\mathrm{PT}} \ll k_{-1} \Rightarrow \frac{\mathrm{d[E]}}{\mathrm{d}t} = -k_2 \times [\mathrm{E}]\,[\mathrm{N}^-] \times \frac{k_{\mathrm{PT}}}{k_{-1}} \quad \text{(very slow proton transfer)} \quad (5)$$

$$\text{with } K = \frac{k_2}{k_{-1}} \Rightarrow \frac{\mathrm{d[E]}}{\mathrm{d}t} = -k_{\mathrm{PT}} \times \mathrm{K} \times [\mathrm{E}]\,[\mathrm{N}^-] \quad (6)$$

In both cases one would observe a monoexponential decay of the electrophile UV/vis-absorbance if one works under pseudo-first-order conditions, and kinetic methods do not allow to differentiate whether the second-order-rate constants $k_{2,\mathrm{obs}}$ listed in Table 3 correspond to k_2 (eq. 1) or $k_{\mathrm{PT}}K$ (eq. 6). The product of $k_{\mathrm{PT}}K$ can be assumed as an apparent rate constant k_{app}.

However, analysis by eq. 1 enables one to differentiate between the both cases. When the log $k_{2,\mathrm{obs}}$-values of Table 3 are plotted against the E-parameters of the electrophiles, one finds that all rate constants for the reactions of **MB** and **ESB** with the electrophiles **1–4**, are on the correlation lines, indicating that eq. 1 holds for these reactions (Figure 3b). As the rate constants for the reactions with **5** and **6** are below the correlation lines, one can assume that these rate constants reflect $k_{\mathrm{PT}}K$.

Analogously, all rate constants for the reactions of **B** and **SB** with **1–4** follow the correlation as expected from eq. 1 (Figure 3a). In contrast to the behavior of **MB** and **ESB**, also the reactions with the quinone methides **6** are on the correlation lines, suggesting that k_2 is measured. In Figure 3a only the $k_{2,\mathrm{obs}}$-values of the reactions with the benzylidene malodinitriles **5** deviate from the linear correlation, indicating that $k_{\mathrm{PT}}K$ is rate-determining in reactions of **B** and **SB** with **5**.

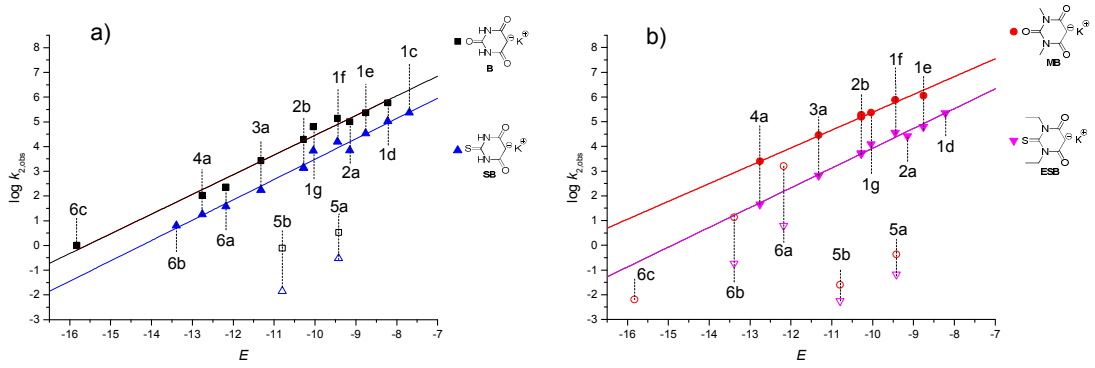

Figure 3. Plots of log $k_{2,obs}$ for the reaction of barbiturate anions with reference electrophiles versus the corresponding electrophilicity parameters E.

Table 2. Second-order-rate constants $k_{2,obs}$ for the reactions of barbiturate anions with electrophiles **1**–**6**, and the resulting nucleophile-specific parameters N and s_N for the barbiturate anions in DMSO at 20 °C.[a)]

Nucleophile	N	s_N	Electrophile	$k_{2,obs}$ [Lmol^{-1}s^{-1}]
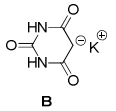 B	15.59	0.80	**1d**	5.90×10^5
			1e	2.33×10^5
			1f	1.26×10^5
			1g	5.28×10^4
			2a	1.01×10^5
			2b	1.93×10^4
			3a	2.69×10^3
			4a	1.05×10^2
			6a	2.31×10^2
			6c	1.14×10^0
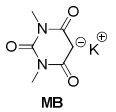 MB	17.46	0.72	**1e**	1.18×10^6
			1f	7.59×10^5
			1g	2.32×10^5
			2b	1.91×10^5
			2b	1.57×10^5
			3a	2.86×10^4
			4a	2.54×10^3
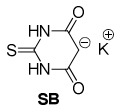 SB	14.24	0.82	**1c**	2.36×10^5
			1d	1.04×10^5
			1e	3.48×10^4
			1f	1.54×10^4
			1g	6.81×10^3
			2a	7.01×10^3
			2b	1.34×10^3
			2b	1.41×10^3
			3a	1.76×10^2
			4a	1.82×10^1
			6a	3.77×10^1
			6b	6.43×10^0
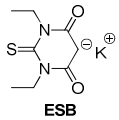 ESB	14.90	0.80	**1d**	2.08×10^5
			1e	6.16×10^4
			1f	3.42×10^4
			1g	1.25×10^4
			2a	2.60×10^4
			2b	5.43×10^3
			2b	5.05×10^3
			3a	6.68×10^2
			4a	4.48×10^1
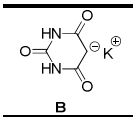 B			**5a**	3.38×10^0
			5b	7.82×10^{-1}
			5c	c)
			6b	b)
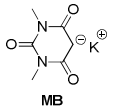 MB			**5a**	4.32×10^{-1}
			5b	2.62×10^{-2}
			5c	c)
			6a	1.62×10^3
			6b	1.38×10^1
			6c	6.46×10^{-3}
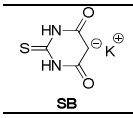 SB			**5a**	1.14×10^{-1}
			5b	1.47×10^{-2}
			5c	c)
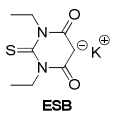 ESB			**5a**	6.62×10^{-2}
			5b	5.60×10^{-3}
			5c	c)
			6a	6.15×10^0
			6b	1.86×10^{-1}

a) The kinetic results of reactions of barbiturate anions with malononitriles **5** and several quinone methide electrophiles **6** are presented separately at the end of the table, because these data were not used for determination of N and s_N. b) no evaluation, because of bisexponential curves; c) no evaluation, because of too slow reaction ($\tau_{1/2} > 48$ h)

Quantum chemical calculations

Although no evidence for the formation of *O*-alkylation products has been found experimentally, quantum chemical calculations have been performed to examine whether initial *O*-attack can account for the deviation of some rate constants from the correlations in Figure 3. The solvent effects for DMSO are included by the COSMO solvation model with $\varepsilon = 48$.

From the quantum chemical investigation, some general features can be derived. The calculated energies and the resulting Gibbs-reaction profiles are exemplarily shown in Figure 4 for the alkylation of **MB** with the neutral electrophiles **2a**, **4a**, **5a**, and **6a**. Obviously for all investigated electrophiles the attack at C(5) is favored over the alkylation at the enolate oxygen (Figure 4). The Gibbs energies of *O*-alkylated products are not only higher than those of the *C*-alkylated products, but also higher than those of the reactants (endergonic reactions). As the transition states for *C*-alkylation are also energetically lower than those for *O*-alkylation (Figure 4), the formation of the *C*-alkylated products is thermodynamically as well as kinetically favored. This result is in accordance with the product studies where only *C*-alkylated products were observed. Therefore, *O*-attack at the barbiturate anion cannot be the reason for the deviations of some reactions from the correlations in Figure 3.

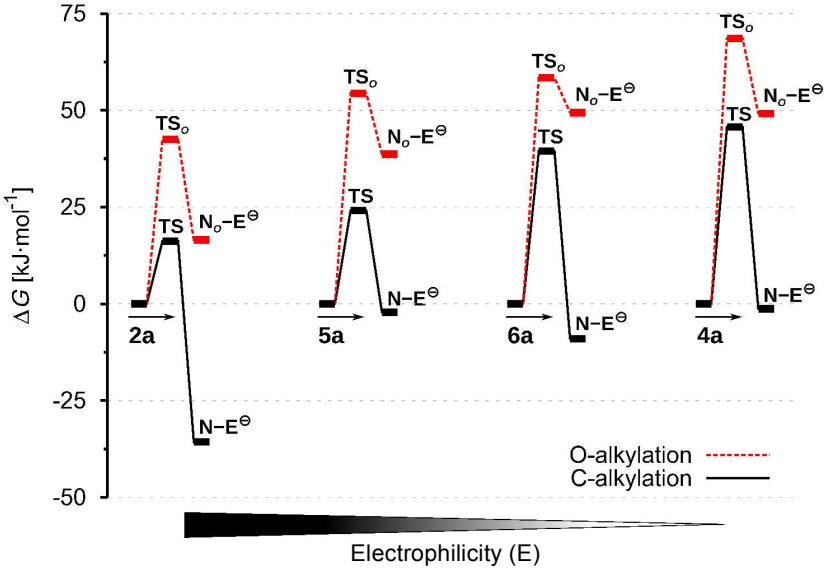

Figure 4. Reaction profiles for the reactions of **MB** at *C*- or at *O*-atom with the electrophiles **2a**, **5a**, **6a**, and **4a**. The transition states for *C*- and *O*-attack as well as the corresponding products are denoted with **TS**/**TS**$_O$ and **N-E**$^{\ominus}$/**N**$_O$**-E**$^{\ominus}$ respectively. The reaction profiles are ordered according to the order of the electrophilicity of the investigated electrophiles. The lowest dispersion complex is set to zero and the energy profiles are given for PW6B95-D3/def2-TZVPP/COSMO single-point calculations (ZPVE: BP86-D3/TZVP).

As shown in Figure 5, the quantum chemically calculated Gibbs-activation energies for the reactions of **B** and **MB** ($\Delta G^{\ddagger}$, open symbols) with neutral electrophiles also correlate linearly with the electrophilicities *E*. This correlation also includes the reactions with electrophiles **5a**–**c** and **6a**,**b**, where the experimentally determined rate constants deviate from the linear correlations shown in Figure 3, i.e., the reactivity order indicated by the *E*-parameters is in full agreement with the quantum chemical calculations of the transition states. This observation provides further evidence for our earlier conclusion (see above) that the deviations from the log k_2 vs. electrophilicity *E* correlations in Figure 3 are due to a change of the rate-determining step.

The lower $\Delta G^{\ddagger}$-values calculated for the reactions of **MB** compared to **B** are in accord with the experimentally observed faster reactions of **MB** (Figure 5). Using the Eyring-equation, the measured second-order-rate constants can be converted into Gibbs-activation energies $\Delta G^{\ddagger}$, which are shown by filled symbols in Figure 5, for the reactions with rate-determining C–C-bond formation.

However, the calculated activation free energies were found to be 15–20 kJmol^{-1} smaller than those derived from the experimentally determined rate constants. This can be attributed to the simplified model in the computational studies (reactant complex as reference point, modeling the solvent environment, etc.). However, as both computational and experimental activation free energies correlate linearly with each other, we can assume that any effects found in the computational study can be transferred to the experimental conditions.

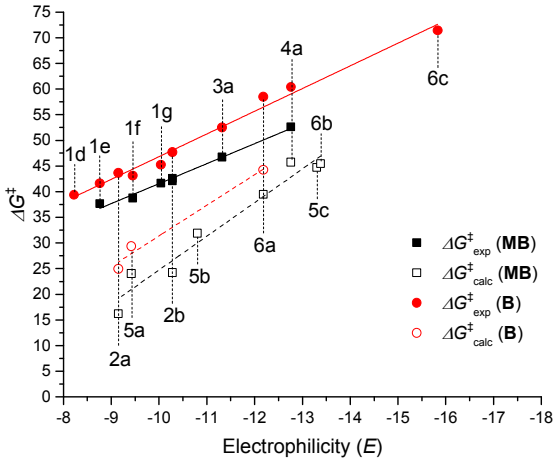

Figure 5. Gibbs-activation energies $\Delta G^{\ddagger}$ (in kJmol^{-1}) derived from the theoretical and the experimental investigation of the reactions of barbiturate anions with reference electrophiles as function of the corresponding electrophilicity parameters *E*.

Discussion

The relative Gibbs energies of the proton transfer products are calculated and compared with the corresponding *C*-alkylated products for the alkylation of **MB** with **2a**, **4a**, **5a**, and **6a** (Figure 6). As shown in Figure 6, the secondary products $^{\ominus}$**N-E**, which results after the alkylation of **MB** with electrophile **5a** or **6a** and the subsequent proton transfer, are energetically favored compared to the initially formed *C*-alkylation product **N-E**$^{\ominus}$. Otherwise, alkylation products **N-E**$^{\ominus}$ for the alkylation of **2a** and **4a** are more stable than the secondary products ($^{\ominus}$**N-E**) which would develop after the proton transfer (Figure 6).

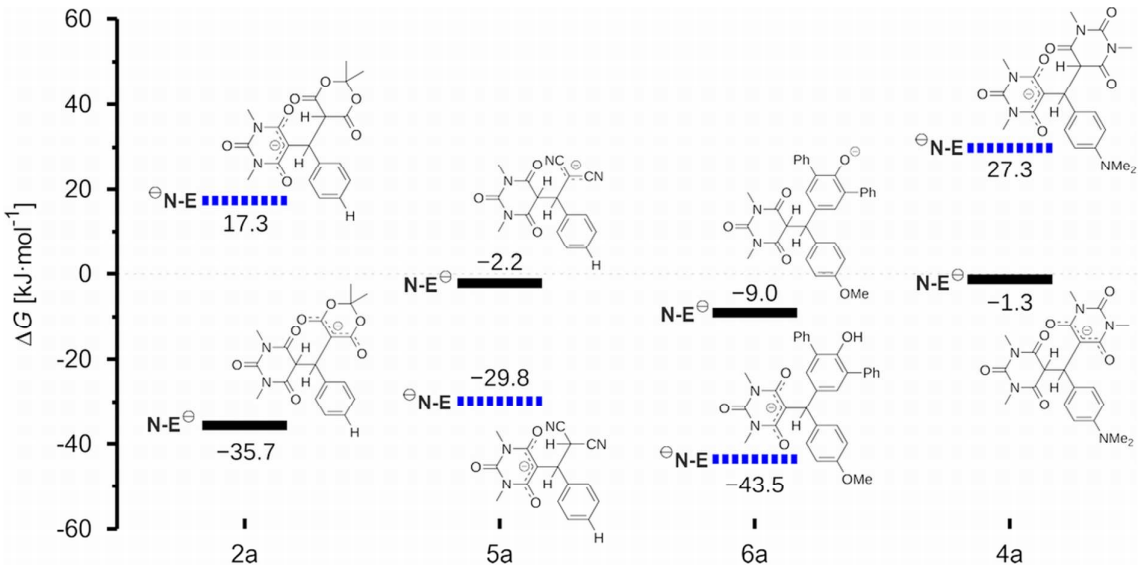

Figure 6. Gibbs-reaction energies Δ*G* for the *C*-alkylation to the product **N-E**$^{\ominus}$ and the subsequent proton transfer (PT) resulting in $^{\ominus}$**N-E** are given for the reaction of **MB** with **2a**, **4a**, **5a**, and **6a**. The energy values are given for PW6B95-D3/def2-TZVPP/COSMO single-point calculations (ZPVE: BP86-D3/TZVP/COSMO).

The interpretation of the product formation for electrophile/barbiturate anion combinations is also possible if the pK_a-values of the parent acids of the intermediates **N-E**$^{\ominus}$ and $^{\ominus}$**N-E** are taken into account (see Table 3). The appropriate scenario is like we illustrated in Scheme 4. The reaction of the electrophile with the barbiturate anion immediately generates **N-E**$^{\ominus}$ which basicity can be reflected by the pK_a of the corresponding parent acids, which were used for discussion, because the actual pK_a-values of **N-E**$^{\ominus}$ are not directly available (Column 3 of Table 3). The structural discrepancy between **N-E**$^{\ominus}$ and the anions of the parent acids seems insignificant for the discussion. The order of pK_a: **6** >> **5** > **4** > **3** > **2** of

the **N-E**$^{\ominus}$-series should not be influenced if consistent functionalization at the electrophilic carbon atom took place, i.e. by reactions with the barbiturate anions **N**$^{\ominus}$.

Now, it can be estimated whether the proton transfer reaction should be of relevance as indicated in Column 4 of Table 3. Obviously, the reactions of electrophiles **5** and **6** with barbiturate anions generate an **N-E**$^{\ominus}$ whose pK_a is greater than that of the barbituric acid itself. That argument readily explains that $^{\ominus}$**N-E** is actually the more thermodynamically stable product compared to **N-E**$^{\ominus}$ when **5** or **6** reacts with a barbiturate anion. As consequence, the consecutive proton transfer reaction can have an effect on the kinetics for those electrophile/nucleophile combinations. Electrophile/nucleophile combinations, which deviate from the linear plot log k_2 as function of E (Figure 3), are specified in the right column of Table 3 for comparison.

Table 3 Parent Brønsted-acid compounds of the Michael acceptor electrophiles **2**, **3**, **4**, **5**, and **6**, pK_a-values in DMSO, theoretically expected scenario when the specific electrophile type reacts with barbiturate anion according to Scheme 10 and indication of electrophile/nucleophile combinations which deviate from the linear plot log $k_{2,obs}$ as function of E.

electrophile type	parent acid	pK_a (DMSO)	expected scenario according to Scheme 10	combinations which show deviating kinetics according to Figure 3
2	 Meldrum's Acid	7.3[54]	no subsequent proton transfer $K_{PT} << 1$	none
3	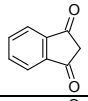 Indandione	7.8[55] DMSO/H_2O (90:10)		none
4	 Barbituric Acid	8.4[54]	an equilibrium state is suggested $K_{PT} \sim 1$	none
5	 Malononitrile	11.0[54]	subsequent proton transfer $K_{PT} >> 1$	**B**, **MB**, **SB**, and **ESB** with **5a**, **5b**, and **5c**
6	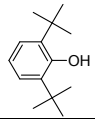 2,6-Di-*tert*-butylphenol	16.8[54]		**MB** with **6a**, **6b**, and **6c**; **ESB** with **6a**, and **6b**

K_{PT} = [$^{\ominus}$**N-E**] / [**N-E**$^{\ominus}$]

It is striking that only such electrophile/nucleophile combinations deviate from the linear plot of log k_2 versus E where $^{\ominus}$**N-E** is the thermodynamically more stable product compared to **N-E**$^{\ominus}$ (Figure 6). Notwithstanding, it is difficult to decide whether k_{-1} or k_{PT} is responsible for the deviating values of k_2, according to eq. 6.

However, due to the clear kinetics of the electrophiles **1**, **2**, **3** and **4**, *N*- and s_N-parameters of the barbiturate anions can be accurately determined according to eq. 1.

Figure 7 shows that the 1,3-dialkylated barbiturates are more nucleophilic than the nonalkylated ones (**MB** > **B** and **ESB** > **SB**). This fact can be explained by the electron-donating effect of the alkyl groups as well as by ground state stabilization of the anions with NH-groups through hydrogen-bonding.[56]

The thiobarbiturates show slightly lower *N*-values than the oxobarbiturates (**SB** < **B**, **ESB** < **MB**), which may be explained by the stronger electron withdrawing effect of the thiocarbonyl group, as indicated by the relative magnitudes of the Hammett-constants of –NH-CO-NH-C_2H_5 (σ_p = –0.26) compared to –NH-CS-NH-C_2H_5 (σ_p = 0.07).[57]

In accordance with the weaker electron-accepting effect of an amidocarbonyl group compared to an alkoxycarbonyl group, the barbituric acid anion **B** (*N* = 15.59) is considerably more nucleophilic than the anion derived from Meldrum's acid (*N* = 13.91), which is comparable to the thiobarbiturate anion **SB** (*N* = 14.24).

Second-order-rate constants of alkylation reactions of 5-methyl-Meldrum's acid and 1,3-dimethylbarbituric acid anions with ethyl iodide in methanol/acetonitrile were determined by Kondo et al.[58] They showed that 1,3-dimethylbarbiturate anion is slightly more nucleophilic than 5-methyl-Meldrum`s acid anion which is substantially in line with our results.

Furthermore, Figure 7 shows that the dimedone anion (*N* = 16.27), where the urea fragment of barbituric acid is replaced by an alkyl group, has a nucleophilicity between **B** and **MB**.

A fair correlation of *N* with pK_{aH} is shown in Figure 8, which includes carbanions of malonic acid derivatives, 1,3-dicarbonyl compounds, and the barbiturate anion **B**. The deviation of cyano-substituted carbanions from this correlation due to the lower reorganization energies has previously been discussed.[28]

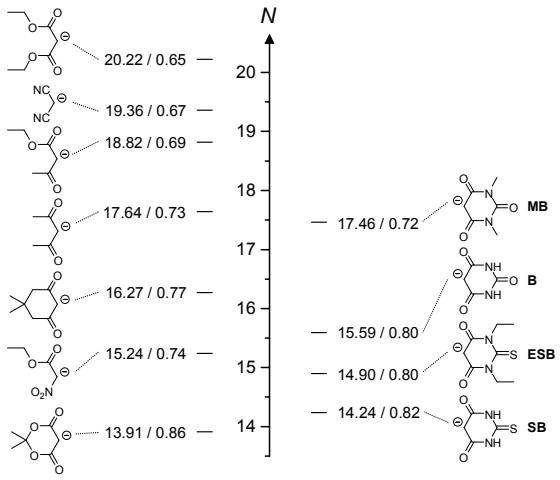

Figure 7. Ranking of the nucleophilicity parameters N/s_N for **B**, **MB**, **SB**, and **ESB** compared to established carbanionic nucleophiles.[59]

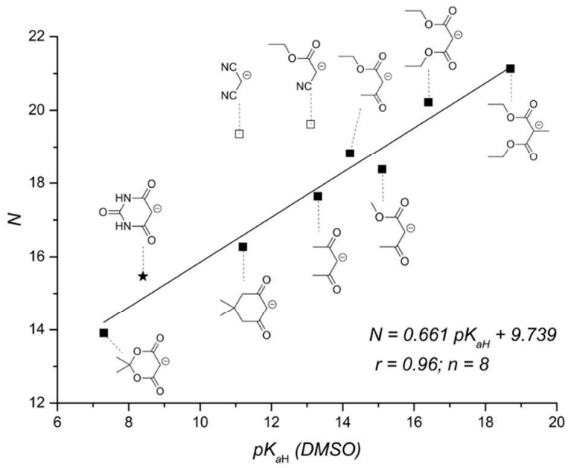

Figure 8. Correlation of the nucleophilicity parameter (N) of carbanions with the pK_a-values of the conjugate acids in DMSO. Sqaures are nucleophilicitie values and acidities of structurally related anions from the literature. The empty squares are cyano-substituted carbanions, which deviate from the linear correlation. The star is the barbituric acid anion (**B**) which nucleophilicity parameter (N) was newly determined.

The discussion of the newly determined nucleophilicity parameters clearly shows that N- and s_N-parameters for barbiturate anions are scientifically sound. Therefore, these data are used according to the methodology already demonstrated in ref. [37] for the thorough discussion of deviant-second-order-rate constants. Now, $k_{2,calcd}$ of the elementary C−C-bond formation step (see Scheme 10 and 11) were calculated from eq. 1 for those electrophile/barbiturate anion combinations for which k_2 is not directly experimentally available using the E-parameters from Table 2 and the just determined N- and s_N-parameters of the barbiturate anions from Table 3. That approach is justified because of the excellent linear correlation of

the electrophilicity parameter E with the quantum-chemically calculated $\Delta G^{\ddagger}$-values (Figure 5).

Calculated $k_{2,calcd}$-value are compiled in Table 4. According to eq. 5 and eq. 6, the desired value of k_{PT}/k_{-1} is the quotient of $k_{2,obs}/k_{2,calcd}$ (Table 4) assuming that $k_{PT} \ll k_{-1}$.

Table 4 Calculated ($k_{2,calcd}$ from eq. 1) and observed ($k_{2,obs}$ from Table 2) second-order-rate constants of electrophile **5** and **6** with barbiturate anion. k_{PT}/k_{-1}-values of Column 4 are charged directly from $k_{2,obs}/k_{2,calcd}$.

N + E-combination	$k_{2,obs}$ (from Table 3) [$Lmol^{-1}s^{-1}$]	$k_{2,calcd}$ (from eq. 1) [$Lmol^{-1}s^{-1}$]	k_{PT} / k_{-1}
B + 5a	3.4×10^{0}	8.6×10^{4}	3.9×10^{-5}
MB + 5a	4.3×10^{-1}	6.2×10^{5}	7.0×10^{-7}
SB + 5a	1.1×10^{-1}	9.0×10^{3}	1.3×10^{-5}
ESB + 5a	6.6×10^{-2}	2.4×10^{4}	2.7×10^{-6}
B + 5b	7.8×10^{-1}	6.8×10^{3}	1.2×10^{-4}
MB + 5b	2.6×10^{-2}	6.2×10^{4}	4.2×10^{-7}
SB + 5b	1.5×10^{-2}	6.6×10^{2}	2.2×10^{-5}
ESB + 5b	5.6×10^{-3}	1.9×10^{3}	2.9×10^{-6}
MB + 6a	1.6×10^{3}	6.3×10^{3}	2.6×10^{-1}
ESB + 6a	6.2×10^{0}	1.5×10^{2}	4.1×10^{-2}
MB + 6b	1.4×10^{1}	8.5×10^{2}	1.6×10^{-2}
ESB + 6b	1.9×10^{-1}	1.6×10^{1}	1.2×10^{-2}
MB + 6c	6.5×10^{-3}	1.5×10^{1}	4.3×10^{-4}

Now, the deviation of the kinetics will be explained more profoundly from data of Table 4. Altogether, k_{PT}/k_{-1} ratios are << 1 of those nucleophile-electrophile-reactions which deviate from the linear plot in Figure 3. This observation clearly confirms that the proton transfer reaction is the rate determining step and not the C−C-bond formation for reactions of electrophile **5** with barbituric anions.

For the electrophiles of type **6** there are differences as function of the structure of the barbiturate anion. Unalkylated barbiturate anions (**B**, **SB**) show a good consistency between $k_{2,obs}$ and $k_{2,calcd}$ (Figure 3b). Only *N*-alkylated barbiturate anions (**MB**, **ESB**) show k_{PT}/k_{-1}-ratios smaller than 1 (Table 4) and those rate constants deviate from the linear correlations in Figure 3a. However, these k_{PT}/k_{-1}-ratios are not as small as found for electrophiles of **5**-type.

A reasonable explanation for that behavior is, that the initially formed intermediates **N-E**$^{\ominus}$ undergo proton transfer more rapidly, if unalkylated barbiturate anions (**B**, **SB**) were used. Tautomerism of the CO–NH moiety might account for this behavior. In case of the *N*-alkylated barbiturate anions (**MB**, **ESB**) the proton transfer is slower and thereby rate determing.

Reasonably, the assumption of the apparent-reaction-rate constant $k_{app} = k_{2,obs} = k_{PT}K$ (eq. 6) for the alkylation with electrophiles of **5**- and some of **6**-type is emphatically substantiated by the considerations in Table 4.

Conclusion

The nucleophilicity parameter N, and the corresponding nucleophile-specific susceptibility parameter s_N for the parent barbiturate **B** (N = 15.59; s_N = 0.80), 1,3-dimethylbarbiturate **MB** (N = 17.46; s_N = 0.72), 2-thiobarbiturate **SB** (N = 14.24; s_N = 0.82), and 1,3-diethyl-2-thiobarbiturate **ESB** (N = 14.90; s_N = 0.80) have been determined from the second-order-rate constants of their reactions with benzhydrylium cations and Michael acceptors. The N-values of the barbiturate anions are in good relationship with the nucleophilicity parameters of related carbanions. In addition, a correlation of N of BA as function of the pK_{aH}-values of the corresponding acids shows the eligibility of the determined nucleophilicity parameters.

The k_2-values for reactions of barbiturate anions with electrophiles of types **1–4** correlated linearly with the electrophilicities E. The corresponding reactions of **MB** and **ESB** with the electrophiles **5** and **6** and of **B** and **SB** with electrophiles **5** were slower than derived from the correlations because the rate-determining step was not the C−C-bond formation but the subsequent proton transfer.

Quantum-chemical calculations show that the product formation during these nucleophile-electrophile-reactions is thermodynamically determined. All calculated activation barriers ($\Delta G^{\ddagger}$) for the C−C-bond-forming step correlate well with the electrophilicity parameters E. This correlation includes also those reactions for which $\Delta G^{\ddagger}$ could not be measured, because C−C-bond formation was not rate-determining. This is the first time that a quantum chemical verification of the empirical E-parameters of electrophiles has been achieved apart from benzhydrylium ions. That approach allows calculation of second-order-rate constants k_2 for such electrophile/barbiturate anion combinations for which only k_{app} is experimentally accessible.

Especially noteworthy is the quantum chemical calculations showed, that *O*-alkylation is kinetically and thermodynamically not favored for the investigated electrophiles. These results are completely in line with the product studies. Nevertheless, *O*-alkylations of BA with alkylhalides[18] or *O*-silylations with hexamethyldisilazane[60] were sometimes reported in the

literature. These examples could be explained by the oxophilicity of the silicon atom or by sterical demanding electrophiles.

Experimental Section

Product studies:

Reaction of **MB** with **1a**:

To a solution of bis(4-tolyl)methylium bromide (74.0 mg 0.269 mmol) in dry DCM, silver triflate (70.0 mg, 0.272 mmol) was added at –80 °C. The solution changes his color to intensive yellow, indicating the formation of the benzhydrylium cation (**1a**). The tetra-*n*-butyl ammonium salt of 1,3-dimethylbarbituric acid (**NBu$_4$MB**) (100 mg, 0.25 mmol) was dissolved in 20 ml DCM and the yellowish solution of bis-tolyl methylium triflate (**1a**) was added under cooling to –80 °C. The reaction was stirred 1 h under cooling, gives 5-(bis-*p*-tolylmethyl)-1,3-dimethylbarbituric acid (**MB1a**). The reaction product was not isolated, because solely *C*-alkylation products were found in the ^{1}H NMR-spectrum of the crude product. Characteristic signals for *O*-alkylation products were not found.

^{1}H NMR (d$_6$-DMSO): δ 2.24 (s, 6H, CH$_3$), 2.94 (s, 6H, CH$_3$), 4.44 (d, $^3J_{HH}$ = 4.5 Hz, 1H, CH), 4.74 (d, $^3J_{HH}$ = 4.5 Hz, 1H, CH), 7.05–7.15 (m, 8H, ArH)

Reaction of **MB** with **1b**:

The reaction is already reported in the literature.[9] The *directly monitored* ^{1}H NMR-experiments confirm the NMR-data from the literature.[9]

^{1}H NMR (d$_6$-DMSO): δ 2.89 (s, 12H, CH$_3$), 2.94 (s, 6H, CH$_3$), 4.33 (d, $^3J_{HH}$ = 4.5 Hz, 1H, CH), 4.61 (d, $^3J_{HH}$ = 4.5 Hz, 1H, CH), 6.74 (d, $^3J_{HH}$ = 7.9 Hz, 4H, ArH), 7.07 (d, $^3J_{HH}$ = 7.9 Hz, 4H, ArH)

Reaction of **MB** with **2b**.

Potassium salt of 1,3-dimethylbarbituric acid (**MB**) (5.0 mg 0.026 mmol) and 2-(4-methoxybenzylidene) meldrum's acid (**2b**) (6.8 mg 0.026 mmol) was dissolved in 1 ml d$_6$-DMSO. ^{1}H NMR-spectra of the solution shows nearly full conversion after few minutes, to give 5-((6-hydroxy-1,3-dimethyl-2,4-dioxo-1,2,3,4-tetrahydropyrimidine-5-yl)(4-

methoxyphenyl)-methyl)-2,2-dimethyl-4-oxo-4*H*-1,3-dioxine-6-olate (**MB2b**) as expected product, as well as two symmetric side products, which were formed by post reactions as described in the results-part. Due to the dynamic equilibria, individual products could not be purely isolated.

^{1}H NMR (d_6-DMSO – Enol): δ 1.57 (s, 6H, CH_3), 3.15 (s, 6H, CH_3), 3.67, 3,69 (s, 3H, CH_3), [5.07 (s, 0.19H), 5.61 (s, 0.39H), 6.12 (s, 0.29H) Σ = 1H, CH], 6.72 (m, 2H, CH), [6.92 (d, $^3J_{HH}$ = 8.50 Hz, 0.69H), 7.01 (d, $^3J_{HH}$ = 8.0 Hz, 0.91H), 7.11 (d, $^3J_{HH}$ = 8.5 Hz, 0.51H) Σ = 2H, CH]

The solution was acidified with trifluoroacetic acid to obtain the neutral compound 6-hydroxy-5-((6-hydroxy-2,2-dimethyl-4-oxo-4*H*-1,3-dioxine-5-yl)(4-methoxyphenyl)methyl)-1,3-dimethylpyrimidine-2,4(1*H*,3*H*)-dione. However, also weak signals of the electrophiles **2b** and **4b** are observed as discussed in the chapter product studies.

^{1}H NMR (d_6-DMSO – Enol): δ 1.56 (s, 6H, CH_3), 3.16 (s, 6H, CH_3), 3.68 (s, 3H, CH_3), 6.12 (s, 1H, CH), 6.71 (d, $^3J_{HH}$ = 7.3 Hz, 2H, ArH), 6.93 (d, $^3J_{HH}$ = 8.3 Hz, 2H, ArH)

Reaction of **MB** with **3a**.

Potassium salt of 1,3-dimethylbarbituric acid (**MB**) (5.0 mg 0.026 mmol) and 2-(4-methoxybenzylidene)indene-1,3-dione (**3a**) (6.8 mg 0.26 mmol) were dissolved in 1 ml d_6-DMSO. The ^{1}H-NMR spectrum of the reactants solution shows nearly complete conversion after few minutes and 2-((1,3-dimethyl-2,4,6-trioxohexahydropyrimidine-5-yl)(4-methoxyphenyl)methyl)-1,3-dioxo-2,3-dihydro-1*H*-indene-2-ide (**MB3a**) is monitored. However, acidification of **MB3a** solution induces a decomposition and formation of **3a** together with 1,3-dimethylbarbituric acid is observed.

^{1}H NMR (d_6-DMSO – Enol): δ 3.12 (s, 6H, CH_3), 3.66 (s, 3H, CH_3), 5.61 (s, 1H, CH), 6.69 (d, $^3J_{HH}$ = 8.5 Hz, 2H, ArH), 6.98 (d, $^3J_{HH}$ = 8.3 Hz, 2H, ArH), 7.20–7.31 (m, 4H, ArH); ^{13}C NMR (d_6-DMSO – Enol): δ 27.7, 28.0, 30.1, 54.9, 91.6, 110.9, 111.9, 113.0, 113.2, 127.8, 135.9, 136.9, 138.2, 151.4, 151.9, 156.7, 163.1

Reaction of **SB** with **4a**.

Potassium salt of 2-thiobarbituric acid (**SB**) (0.663 mg, 0.004 mmol) was dissolved in 1 ml d_6-DMSO. 5-(4-dimethylamino)benzylidene-1,3-dimethylbarbituric acid (**4a**) (1.023 mg,

0.004 mmol) dissolved in 1 ml d_6-DMSO was added. The ^{1}H NMR-spectrum of the solution shows about 60 % conversion of the reactants after few minutes. 5-(4-dimethylamino)phenyl)(2-thiobarbiturate)methyl)-1,3-dimethylbarbiturate (**SB4a**) is observed as expected product, as well as two side products, which were formed by post reactions as described in the chapter products studies. Due to the dynamic equilibria, individual products could not be purely isolated as subsequently demonstrated.

^{1}H NMR (d_6-DMSO – Enol): δ 2.79 (s, 6H, CH_3), 2.99 (s, 6H, CH_3), [5.86 (s, 0.12H), 5.98 (s, 0.44H), 6.09 (s, 0.40H) Σ 1H, CH], 6.55 (d, $^3J_{HH}$ = 8.8 Hz, 2H, ArH), 6.82 (d, $^3J_{HH}$ = 9.0 Hz, 2H, ArH), [11.40 (s), 11.52 (s), 11.53 (s) Σ 2H, NH]

The solution was acidified with trifluoroacetic acid to obtain the neutral compound 5-((4-(dimethylamino)phenyl)(6-hydroxy-4-oxo-2-thio-1,2,3,4-tetrahydropyrimidine-5-yl)methyl)-6-hydroxy-1,3-dimethylpyrimidine-2,4(1*H*,3*H*)-dione. Additionally, 5-(4-dimethylamino)benzylidene-1,3-dimethylbarbituric acid (**4a**) as well as 5-(4-dimethylamino)benzylidene-2-thioxobarbituric acid was obtained.

^{1}H NMR (d_6-DMSO – Enol): δ 3.10 (s, 6H, CH_3), 3.12 (s, 6H, CH_3), 5.99 (s, 1H, CH), 7.19 (d, $^3J_{HH}$ = 7.8 Hz, 2H, ArH), 7.50 (d, $^3J_{HH}$ = 8.8 Hz, 2H, ArH), 11.71 (m, 2H, NH).

Reaction of **MB** with **5a**:

Potassium salt of 1,3-dimethylbarbituric acid (**MB**) (76.2 mg, 0.392 mmol) was dissolved in 5 ml DMSO under slight heating. Benzylidenemalononitrile (**5a**) (60.5 mg, 0.392 mmol), also dissolved in 5 ml DMSO, was added and stirred at room temperature for 2 h. The ^{1}H NMR-spectrum of the combined solutions shows nearly complete conversion to 5-(2,2-dicyano-1-phenylethyl)-1,3-dimethylbarbiturate (**MB5a**) as intermediate product.

^{1}H NMR (d_6-DMSO): δ 3.07 (s, 6H, CH_3), 4.69 (d, $^3J_{HH}$ = 12.3 Hz, 1H, CH), 6.20 (d, $^3J_{HH}$ = 12.3 Hz, 1H, CH), 7.18–7.28 (m, 3H, ArH), 7.52 (d, $^3J_{HH}$ = 7.0 Hz, 2H, ArH); ^{13}C NMR (d_6-DMSO): δ 25.7, 26.8, 43.7, 83.4, 115.0, 115.3, 126.6, 127.8, 127.9, 141.8, 152.6, 161.8

After acidification with trifluoroacetic acid, the DMSO solution was poured into 50 ml water and extracted twice with 30 ml DCM. The combined organic phases were dried over $MgSO_4$ and the solvent was evaporated The obtained solid was 7-amino-1,3-dimethyl-2,4-dioxo-5-phenyl-2,3,4,5-tetrahydro-1*H*-pyrano[2,3-*d*]pyrimidine-6-carbonitrile (**MB5aH**)[11,61] with one equivalent DMSO (116 mg, 0.299 mmol, 76 %)

melting point: 230−233 °C; ^{1}H NMR (d_6-DMSO): δ 3.08 (s, 3H, CH_3), 3.36 (s, 3H, CH_3), 4.33 (s, 1H, CH), 7.20−7.33 (m, 7H, ArH, NH_2); ^{13}C NMR (d_6-DMSO): δ 27.7, 29.2, 36.6, 58.7, 88.9, 119.1, 126.8, 127.4, 128.3, 144.2, 150.1, 151.2, 157.7, 160.5

Reaction of **MB** with **5c**.

Potassium salt of 1,3-dimethylbarbituric acid (**MB**) (97.0 mg, 0.499 mmol) was dissolved in 5 ml DMSO under slight heating. 4-Dimethylamino-benzylidene malononitrile (**5c**) (99.0 mg, 0.502 mmol), also dissolved in 5 ml DMSO, was added and stirred at room temperature for 30 h. The ^{1}H NMR-spectrum of the combined solutions shows about 50 % conversion of the reactants. Therefore, the solution was heated up to 100 °C for 8 h and stirred 24 h at room temperature to produce 5-(2,2-dicyano-1-(4-dimethylaminophenyl)ethyl)-1,3-dimethylbarbiturate (**MB5c**) in sufficient amount for a clear ^{1}H NMR-analysis. However, acidification of **MB5c** leads to a decomposition and the formation of **5c** together with 1,3-dimethylbarbituric acid.

^{1}H NMR (d_6-DMSO): δ 2.83 (s, 6H, CH_3), 3.07 (s, 6H, CH_3), 4.57 (d, $^3J_{HH}$ = 12.3 Hz, 1H, CH), 6.11 (d, $^3J_{HH}$ = 12.0 Hz, 1H, CH), 6.60 (d, $^3J_{HH}$ = 8.8 Hz, 2H, ArH), 7.33 (d, $^3J_{HH}$ = 8.8 Hz, 2H, ArH); ^{13}C NMR (d_6-DMSO): δ 26.2, 26.9, 40.3, 43.2, 84.0, 112.1, 115.3, 115.6, 128.5, 129.7, 149.4, 152.7, 161.8

Reaction of **B** with **6c**.

Potassium salt of barbituric acid (**B**) (0.5 mg 0.003 mmol) and 2,6-di-*tert*-butyl-4-(4-methylbenzylidene)-cyclohexa-2,5-dienone (**6c**) (0.8 mg 0.003 mmol) were dissolved in 1 ml d_6-DMSO. The ^{1}H NMR-spectrum of the solution shows nearly complete conversion of the reactants after few minutes and 5-((3,5-di-*tert*-butyl-4-hydroxyphenyl)(4-tolyl)methyl)-barbiturate (**B6c**) is monitored.

^{1}H NMR (d_6-DMSO): δ 1.30 (s, 18H, CH_3), 2.22 (s, 3H, CH_3), 5.21 (s, 1H, CH), 6.88 (d, $^3J_{HH}$ = 8.3 Hz, 2H, ArH), 7.05 (d, $^3J_{HH}$ = 8.0 Hz, 2H, ArH), 7.15 (s, 2H, ArH), 8.62 (s, 2H, NH)

Reaction of **MB** with **6c**.

Potassium salt of 1,3-dimethylbarbituric acid (**MB**) (5.0 mg 0.026 mmol) and 2,6-di-*tert*-butyl-4-(4-methylbenzylidene)-cyclohexa-2,5-dienone (**6c**) (7.9 mg 0.026 mmol) were dissolved in 1 ml d_6-DMSO. The ^{1}H NMR-spectrum of the solution shows nearly complete conversion of the reactants after few minutes and 5-((3,5-di-*tert*-butyl-4-hydroxyphenyl)(4-tolyl)methyl)-1,3-dimethylbarbiturate (**MB6c**) is monitored.

^{1}H NMR (d_6-DMSO): δ 1.30 (s, 18H, CH_3), 2.20 (s, 3H, CH_3), 3.01 (s, 6H, CH_3), 5.34 (s, 1H, CH), 6.42 (s, 1H, OH), 6.88 (d, $^3J_{HH}$ = 7.8 Hz, 2H, ArH), 7.04 (d, $^3J_{HH}$ = 7.8 Hz, 2H, ArH), 7.14 (s, 2H, ArH); ^{13}C NMR (d_6-DMSO): δ 20.7, 27.0, 30.7, 34.4, 46.0, 88.9, 125.6, 127.4, 137.1, 137.5, 144.7, 128.6, 132.3, 150.8, 153.1, 161.8

Potassium salt of 1,3-dimethylbarbituric acid (**MB**) (97.0 mg 0.499 mmol) and 2,6-di-*tert*-butyl-4-(4-methylbenzylidene)-cyclohexa-2,5-dienone (**6c**) (150.0 mg 0.486 mmol) were dissolved in 3 ml DMSO. The reaction was stirred for 2 h at room temperature. Then, 10 ml 1 M HCl was added and a yellow solid precipitates. The solid was filtered off, washed with water and dried under reduced pressure. As product 0.210 g (0.452 mmol, 93 %) of 5-((3,5-di-*tert*-butyl-4-hydroxyphenyl)(4-tolyl)methyl)-1,3-dimethylbarbituric acid (**MB6cH**) was obtained as pale yellow powder.

melting point: 157−159 °C; ^{1}H NMR (d_6-DMSO): δ 1.29 (s, 18H, CH_3), 2.27 (s, 3H, CH_3), 2.83 (s, 3H, CH_3), 2.97 (s, 3H, CH_3), 4.29 (d, $^3J_{HH}$ = 2.5 Hz, 1H, CH_3), 4.63 (d, $^3J_{HH}$ = 2.5 Hz, 1H, CH_3), 6.82 (s, 2H, ArH), 7.11 (d, $^3J_{HH}$ = 8.0 Hz, 2H, ArH), 7.29 (d, $^3J_{HH}$ = 8.0 Hz, 2H, ArH); ^{13}C NMR (d_6-DMSO): δ 20.6, 27.8, 28.0, 30.2, 34.4, 40.0, 54.4, 124.7, 128.3, 128.6, 129.8, 135.6, 137.8, 138.9, 151.0, 152.9, 167.9, 169.0; Anal. Calcd for $C_{28}H_{36}N_2O_4$: C: 72.39; H: 7.81; N: 6.03. Found: C: 72.34; H: 7.69; N: 6.02.

Kinetics:

The studied barbiturate anions were used as potassium salts, all kinetics were measured in dry DMSO (Acros, H_2O < 0.005%) at 20 °C and monitored by UV/vis spectroscopy. The used UV/vis absorption maxima are given in Table 1. The addition of 1.3 equivalents of 18-crown-6 did not change the obtained $k_{2,obs}$-values, indicating that the corresponding cations have no influence on the kinetics.

Fast reactions with $\tau_{1/2}$ < 100 s were investigated with stopped flow technique, slower reactions were measured with standard UV/vis equipment.

Instruments and Materials:

NMR-spectra were measured on a 250 MHz (^{1}H) and 62.9 MHz (^{13}C) device. Chemical shifts are given in ppm and refer to TMS (δ_H = 0.00 ppm). Electrophiles **1a** and **1b**,[47,62] **2a** and **2b**,[63] **3a**,[41] **4a**,[64] as well as **5a**, **5b**, and **5c**[65] for product studies were prepared according to the literature. The used barbiturate anions were prepared by treatment of the barbituric acids with K_2CO_3 or tetra-*n*-butylammonium hydroxide in water and recrystallization.

Computational Details:

All quantum chemical calculations were performed using the TURBOMOLE 6.5[66] quantum chemistry program package. The potential energy surface (PES) for each reaction was explored using the density functional theory (DFT). We used BP86[67-70] functional with Grimme's dispersion correction (D3)[71] and TZVP[72-74] basis. The equilibrium structures and the transition state structures were confirmed by normal-mode analysis.[75] For the BP86-D3/TZVP geometry optimized structures single-point energies were calculated more accurately. Therefore, several common functionals like PBE0,[67,76-78] TPSS,[67,76,78,79] TPSSH[67,76,78-80] and PW6B95[81] with D3 correction and def2-TZVPP[82,83] basis set were employed (see SI page S29 – S77). The results obtained by the sophisticated PW6B95 functional were chosen for a detailed discussion. Solvent effects were included by applying the COSMO[84] solvation model with ε = 48 (for DMSO as solvent). The Gibbs energies were calculated by `freeh` module as implemented in TURBOMOLE 6.5 (see SI page S29 – S77). The reported relative Gibbs energies (ΔG) and the activation barriers ($\Delta G^{\ddagger}$) are given in kJ mol^{-1}.

Acknowledgement

The authors thank Prof. Herbert Mayr for the opportunity measuring the reaction kinetic at his devices at the LMU in Munich and the intense discussions and support writing this paper. The DFG (Deutsche Forschungsgemeinschaft SP 392/26-1 and 26-3) is gratefully acknowledged for financial support. Furthermore, we thank the Technische Universität Chemnitz for providing computing time on the computation cluster CHiC. Joachim Friedrich also thanks the Fonds der Chemischen Industrie for financial support due to the Material Cost Allowances program.

Supporting Information Available

All kinetic data, NMR spectra and data from DFT calculations are summarized in the Supporting Information. This material is available free of charge via the Internet at http://pubs.acs.org.

(1) Dilger, J. P.; Boguslavsky, R.; Barann, M.; Katz, T.; Vidal, A. M. *J. Gen. Physiol.* **1997**, *109*, 401.

(2) Piloty, O. *Liebigs Ann. Chem.* **1904**, *333*, 22.

(3) Brooker, L. G. S.; Craig, A. C.; Heseltine, D. W.; Jenkins, P. W.; Lincoln, L. L. *J. Am. Chem. Soc.* **1965**, *87*, 2443.

(4) Seifert, S.; Seifert, A.; Brunklaus, G.; Hofmann, K.; Ruffer, T.; Lang, H.; Spange, S. *New J. Chem.* **2012**, *36*, 674.

(5) Zatsikha, Y. V.; Yakubovskyi, V. P.; Shandura, M. P.; Kovtun, Y. P. *RSC Adv.* **2013**, *3*, 24193.

(6) Dickey, J. B.; Grey, A. R. *Org. Synth.* **1943**, *2*, 60.

(7) Moskvin, A. V.; Reznikova, N. R.; Ivin, B. A. *Russ. J. Org. Chem.* **2002**, *38*, 463.

(8) Jursic, B. S.; Neumann, D. M.; Bowdy, K. L.; Stevend, E. D. *J. Heterocyclic Chem.* **2004**, *41*, 233.

(9) Bauer, M.; Spange, S. *Eur. J. Org. Chem.* **2010**, 259.

(10) Krasnaya, Z. A.; Kachala, V. V.; Zlotin, S. G. *Mendeleev Commun.* **2014**, *24*, 377.

(11) Seeliger, F.; Berger, S. T. A.; Remennikov, G. Y.; Polborn, K.; Mayr, H. *J. Org. Chem.* **2007**, *72*, 9170.

(12) Schade, A.; Schreiter, K.; Rüffer, T.; Lang, H.; Spange, S. *Chem. Eur. J.* **2016**, *22*, 5734.

(13) Bolz, I.; Spange, S. *Chem. Eur. J.* **2008**, *14*, 9338.

(14) Jursic, B. S. *J. Heterocyclic Chem.* **2001**, *38*, 655.

(15) Jursic, B. S.; Neumann, D. M.; Moore, Z.; Stevens, E. D. *J. Org. Chem.* **2002**, *67*, 2372.

(16) Maas, G.; Weber, H.-M. *Tetrahedron* **1985**, *41*, 4529.

(17) Feith, B.; Weber, H.-M.; Maas, G. *Liebigs Ann. Chem.* **1986**, *1986*, 2123.

(18) Krasnov, K. A.; Slesarev, V. I.; Artemava, Z. L. *Zh. Org. Khim.* **1989**, *25*, 1553.

(19) Krasnov, K. A.; Slesarev, V. I. *Russ. J. Org. Chem.* **1997**, *33*, 543.

(20) Neville, G. A.; Avdovich, H. W. *Can. J. Chem.* **1972**, *50*, 880.

(21) Aspelund, H. *J. Prakt. Chem.* **1933**, *137*, 1.

(22) Berggårdh, C. *Acta Acad. Abo., Ser. B* **1935**, *9*, No. 3.

(23) Briggs, A. G.; Sawbridge, J. E.; Tickle, P.; Wilson, J. M. *J. Chem. Soc. B* **1969**, 802.

(24) Koffer, H. *J. Chem. Soc., Perkin Trans. 2* **1974**, 1428.

(25) Masoud, M. S.; Soliman, E. M.; Elkholy, A. E.; Khalil, E. A. *Thermochim. Acta* **1988**, *136*, 1.

(26) Medien, H. A. A.; Zahran, A. A. *Spectrochim. Acta A* **2001**, *57*, 2505.

(27) Lucius, R.; Loos, R.; Mayr, H. *Angew. Chem. Int. Ed.* **2002**, *41*, 91.

(28) Bug, T.; Mayr, H. *J. Am. Chem. Soc.* **2003**, *125*, 12980.

(29) Lucius, R.; Mayr, H. *Angew. Chem. Int. Ed.* **2000**, *39*, 1995.

(30) Bug, T.; Lemek, T.; Mayr, H. *J. Org. Chem.* **2004**, *69*, 7565.

(31) Phan, T. B.; Mayr, H. *Eur. J. Org. Chem.* **2006**, 2530.

(32) Berger, S. T. A.; Ofial, A. R.; Mayr, H. *J. Am. Chem. Soc.* **2007**, *129*, 9753.

(33) Seeliger, F.; Mayr, H. *Org. Biomol. Chem.* **2008**, *6*, 3052.

(34) Kaumanns, O.; Appel, R.; Lemek, T.; Seeliger, F.; Mayr, H. *J. Org. Chem.* **2009**, *74*, 75.

(35) Corral-Bautista, F.; Mayr, H. *Eur. J. Org. Chem.* **2013**, 4255.

(36) Chen, X.; Tan, Y.; Berionni, G.; Ofial, A. R.; Mayr, H. *Chem. Eur. J.* **2014**, *20*, 11069.

(37) Corral-Bautista, F.; Mayr, H. *Eur. J. Org. Chem.* **2015**, 7594.

(38) Corral-Bautista, F.; Klier, L.; Knochel, P.; Mayr, H. *Angew. Chem. Int. Ed.* **2015**, *54*, 12497.

(39) Mayr, H.; Kempf, B.; Ofial, A. R. *Accounts Chem. Res.* **2003**, *36*, 66.

(40) Richter, D.; Hampel, N.; Singer, T.; Ofial, A. R.; Mayr, H. *Eur. J. Org. Chem.* **2009**, *2009*, 3203.

(41) Berger, S. T. A.; Seeliger, F. H.; Hofbauer, F.; Mayr, H. *Org. Biomol. Chem.* **2007**, *5*, 3020.

(42) Lemek, T.; Mayr, H. *J. Org. Chem.* **2003**, *68*, 6880.

(43) Mayr, H.; Bug, T.; Gotta, M. F.; Hering, N.; Irrgang, B.; Janker, B.; Kempf, B.; Loos, R.; Ofial, A. R.; Remennikov, G.; Schimmel, H. *J. Am. Chem. Soc.* **2001**, *123*, 9500.

(44) Kaumanns, O.; Mayr, H. *J. Org. Chem.* **2008**, *73*, 2738.

(45) Baidya, M.; Mayr, H. *Chem. Comm.* **2008**, 1792.

(46) Kaumanns, O.; Lucius, R.; Mayr, H. *Chem. Eur. J.* **2008**, *14*, 9675.

(47) Breugst, M.; Mayr, H. *J. Am. Chem. Soc.* **2010**, *132*, 15380.

(48) Bernasconi, C. F.; Fornarini, S. *J. Am. Chem. Soc.* **1980**, *102*, 5329.

(49) Schmid, R.; Sapunov, V. N. *Non-Formal Kinetics*; Verlag Chemie: Weinheim, 1982.

(50) Li, Z.; Chen, Q.; Mayer, P.; Mayr, H. *J. Org. Chem.* **2017**, *82*, 2011.

(51) House, J. E. *Principles of Chemical Kinetics*; WCB-Publishing: Dubuque, 1997.

(52) Kehlen, H.; Kuschel, F.; Sackmann, H. *Grundlagen der Chemischen Kinetik*; Akademie-Verlag: Berlin, 1974.

(53) Logan, S. R. *Grundlagen der Chemischen Kinetik*; Wiley-VCH: Weinheim, 1997.

(54) Bordwell, F. G. *Accounts Chem. Res.* **1988**, *21*, 456.

(55) Bernasconi, C. F.; Paschalis, P. *J. Am. Chem. Soc.* **1986**, *108*, 2969.

(56) Hansch, C.; Leo, A.; Taft, R. W. *Chem. Rev.* **1991**, *91*, 165.

(57) Nishiguchi, T.; Iwakura, Y. *J. Org. Chem.* **1970**, *35*, 1591.

(58) Kondo, Y.; Yano, K.; Urade, M.; Yamada, A.; Kouyama, R.; Takagi, T. *J. Chem. Soc., Perkin Trans. 2* **1999**, 1181.

(59) http://www.cup.lmu.de/oc/mayr/reaktionsdatenbank 04.12.2015.

(60) Studentsov, E. P.; Kokhanovskii, A. N.; Ganina, M. B.; Nikolaeva, N. I.; Fedorova, E. V.; Moskvin, A. V.; Ivin, B. A. *Rus. J. Gen. Chem.* **2004**, *74*, 261.

(61) Shaabani, A.; Simadi, S.; Rahmati, A. *Synth. Comm.* **2007**, *37*, 491.

(62) Padmaaban, M.; Akkattu, T. B.; Glorius, F. *Org. Lett.* **2011**, *13*, 98.

(63) Sandhu, H. S.; Sapra, S.; Gupta, M.; Nepali, K.; Gautam, R.; Yadav, S.; Kumar, R.; Jachak, S. M.; Chugh, M.; Gupta, M. K.; Suri, O. P.; Dhar, K. L. *Bioorg. Med. Chem.* **2010**, *18*, 5626.

(64) Figueroa-Villar, J. D.; Vieira, A. A. *J. Mol. Struct.* **2013**, *1034*, 310.

(65) Mantri, M.; Graaf, O. d.; Veldhoven, J. v.; Göblyös, A.; Künzel, J. K. v. F. D.; Mulder-Krieg, T.; Link, R.; Vries, H. d.; Beukers, M. W.; Brussee, J.; Ijzerman, A. P. *Promo/Aldehyd* **2008**, *51*, 4449.

(66) University of Karlsruhe and Forschungszentrum Karlsruhe GmbH, 1989-2007, TURBOMOLE GmbH, since 2007: available from http://www.turbomole.com, 2013.

(67) Slater, J. C. *Phys. Rev.* **1951**, *81*, 385.

(68) Becke, A. D. *Phys. Rev. A* **1988**, *38*, 3098.

(69) Vosko, S. H.; Wilk, L.; Nusai, M. *Can. J. Chem.* **1980**, *58*, 1200.

(70) Perdew, J. P. *Phys. Rev. B* **1986**, *33*, 8822.

(71) Grimme, S.; Anthony, J.; Ehrlich, S.; Krieg, H. *J. Chem. Phys.* **2010**, *132*, 154104.

(72) Eichkorn, K.; Treutler, O.; Öhm, H.; Häser, M.; Ahlrichs, R. *Chem. Phys. Lett.* **1995**, *242*, 652.

(73) Eichkorn, K.; Weigend, F.; Treutler, O.; Ahlrichs, R. *Theor. Chem. Acc.* **1997**, *97*, 119.

(74) Schaefer, A.; Huber, C.; Ahlrichs, R. *J. Chem. Phys.* **1994**, *100*, 5829.

(75) Deglmann, P.; Furche, F.; Ahlrichs, R. *Chem. Phys. Lett.* **2002**, *362*, 511.

(76) Dirac, P. A. M. *Proc Royal. Soc. (London) A* **1929**, *123*, 714.

(77) Perdew, J. P.; Burke, K.; Ernzerhof, M. *Phys. Rev. Lett.* **1996**, *77*, 3865.

(78) Perdew, J. P.; Yang, W. *Phys. Rev. B* **1992**, *45*, 13244.

(79) Tao, J. M.; Perdew, J. P.; Staroverov, V. N.; Scuseria, G. E. *Phys. Rev. Lett.* **2003**, *91*, 146401.

(80) Staroverov, V. N.; Scuseria, G. E.; Tao, J. M.; Perdew, J. P. *J. Chem. Phys.* **2003**, *119*, 12129.

(81) Zhao, Y.; Truhlar, D. G. *J. Phys. Chem. A* **2005**, *109*, 5656.

(82) Weigend, F. *Phys. Chem. Chem. Phys.* **2006**, *8*, 1057.

(83) Weigend, F.; Furche, F.; Ahlrichs, R. *J. Chem. Phys.* **2003**, *119*, 12753.

(84) Klamt, A.; Schüürmann, G. *J. Chem. Soc., Perkin Trans. 2* **1993**, 799.